

## Radiative power and x-ray spectrum numerical estimations for wire array Z-pinches

This content has been downloaded from IOPscience. Please scroll down to see the full text.

2015 J. Phys.: Conf. Ser. 653 012148

(<http://iopscience.iop.org/1742-6596/653/1/012148>)

View [the table of contents for this issue](#), or go to the [journal homepage](#) for more

Download details:

IP Address: 90.154.66.112

This content was downloaded on 12/11/2015 at 07:30

Please note that [terms and conditions apply](#).

# Radiative power and x-ray spectrum numerical estimations for wire array Z-pinches

O G Olkhovskaya<sup>1</sup>, M M Basko<sup>1</sup>, P V Sasorov<sup>1</sup>, I Yu Vitchev<sup>1</sup>,  
V G Novikov<sup>1</sup>, A S Boldarev<sup>1</sup>, V A Gasilov<sup>1</sup> and S I Tkachenko<sup>2,3</sup>

<sup>1</sup> Keldysh Institute of Applied Mathematics of the Russian Academy of Sciences, Miusskaya Square 4, Moscow 125047, Russia

<sup>2</sup> Moscow Institute of Physics and Technology, Institutskiy Pereulok 9, Dolgoprudny, Moscow Region 141700, Russia

<sup>3</sup> Joint Institute for High Temperatures of the Russian Academy of Sciences, Izhorskaya 13 Bldg 2, Moscow 125412, Russia

E-mail: boldar@imamod.ru

**Abstract.** Magnetically driven plasma implosion is studied numerically with the use of a 3D radiative MHD model. We consider a Z-pinch formed by an array of thin tungsten wires. In our calculations we take into account a time-extended plasma production due to a material evaporation by an individual wire caused by the heating electric current. Using a detailed model of the pinch kernel, a soft x-ray radiation intensity is analyzed numerically with resolution of temporal, spatial, angular and spectral radiation characteristics. The results are represented for the conditions pertinent to experiments with cylindrical tungsten wire arrays at Angara-5-1 facility (TRINITI, RF).

## 1. Introduction

Experiments carried out in the middle of 90-th with wire arrays (including tens or hundreds micron-size wires) taken as loads for high-current nanosecond pulse generators demonstrated an increase of a hydromagnetic stability in Z-pinch plasmas. Consequently, it was observed a shortening of x-ray pulse duration while preserving a radiation energy output integrated over a spectrum corresponding to the imploded matter. Low-inductance facilities having a current rise-time  $\sim 100$  ns can provide up to  $\sim 6$  ns duration soft x-ray pulse with very high coefficient of kinetic energy conversion into a thermal radiation in the imploding plasma. A radiation power in soft x-ray band ( $\sim 100$ – $200$  eV) is about 5–7 TW in experiments done at Angara-5-1 facility (TRINITI, RF) while peak current value reaches  $\sim 4$  MA.

Diagnostic tools used at Angara-5-1 allow measurements of soft x-ray spectra resolved in angles and time [1]. There exists a possibility of getting temporally resolved filtered pinch images at a moment of “main” x-ray pulse. Considering a problem of processing these experimental data we have to develop a model of unsteady soft x-ray spectra produced by a pinch kernel. This model should account for spatial and angular radiation intensity resolution.

The purpose of the present work is to study 3D structures inherent to a strongly radiating pinch. To this end, we use numerical data obtained by means of a radiative MHD code MARPLE (KIAM RAS, [2]). An existing MARPLE version calculates a radiative transfer via a multigroup



diffusion model. Therefore our 3D simulations can give us unsteady spectra, however without information concerning spatial and angular photon distributions.

Intensive plasma shell deceleration at the pinch axis is accompanied by supercritical radiating shock wave [3]. At the shock front, a kinetic energy of the shell is converted into a radiation energy. It is essential that the great portion of radiation is generated in the x-band. The radiation regenerates in a narrow zone with a micron-size thickness and then leaves a plasma domain. This effect can be reproduced in simulations using the code MARPLE. However today an available computational meshes are not so fine as to correspond to a spatial resolution level needed for correct simulation of the mentioned hot zone placed after a supercritical shock front. Therefore the details in a Z-pinch spectrum definitely pertinent to this hot region are absent in spectral distributions calculated via MARPLE. One of these details is a distinct “tail” in a hard x-ray spectral band observed in experiments at Z-machine (SNL, USA), e. g. see [4]. We have reasons to believe that under the Angara-5-1 conditions such “tail” is relatively more bright, however a main portion of x-pulse energy relates to more soft quanta.

Due to “multiphysics” character and some drawbacks of modern multiscale radiative MHD modeling a lot of fast Z-pinch studies are carried out via simplified pinch models. These models do not serve for a complete and detailed implosion description, instead, they are concentrated on the physics of plasmas compressed into a “kernel” near the pinch axis. Obviously this approach causes a “splitting” between the physics of implosion and the physics of the stagnated (final stage) pinch.

In [3] a real pinch spectra are compared with those produced by a tungsten plasmas with constant temperature and homogeneously distributed over inside a round cylinder. Herewith a soft x-radiation emission, absorption and transfer is calculated in correlation with ionization processes and populations of atomic levels according to a model [5]. The results presented in our paper are gained in numerical experiments with MHD models equipped with equation of state, emissivity and opacity data tables built through application of a technique [6] and the code THERMOS (KIAM RAS).

## 2. Models and methods for fast Z-pinch simulations

A Z-pinch discussed here presents the cylindrical wire array. To describe a plasma motion we use a coupled model including equations of magnetohydrodynamics and radiative transfer phenomena. A thermal radiation produced by a pinch plasma is described by a multigroup diffusion model. Usually to implement radiative MHD calculations we use emissivity/opacity data tables with 36 spectral groups. This is quite satisfactory approximation to plasma spectra allowing reproduce a radiation-matter energy balance with appropriate accuracy.

The description of the initial stage of the heating of individual wire and as a result the plasma ablation has fundamental importance for the simulations of the wire array dynamics. The complete theoretical description of the so-called “cold start”, i. e., the dynamics of material of the exploded wire starting with its solid state, is a very complicated problem. This problem is still in the stage of active studying and development [7], therefore now as a rule, different semi-empirical models are used in simulations. In the presented numerical simulations the plasma generation is described by the semi-empirical model of the protracted formation of plasma [8]. This model was adjusted to experiments with multiwire arrays at ANGARA-5-1 facility. The model [8] takes into account Joule heating of hot plasma in the flow and transport of the deposited energy toward relatively cold condensed part of existing yet wires. This transport is caused by electron thermal conduction and by radiation.

A realistic model of a wire array electric explosion [8] describes correctly a formation of a “pre-pinch” or “precursor” structure distinctively observed in experiments. Computer simulations using the model [8] give plasma parameter distributions adequate to experimental data.

### 3. 3D MHD modeling of a wire array Z-pinch

We analyse the data obtained in the typical Angara-5-1 shot No. 4847. The paper [5] gives the corresponding results of measurements regarding to plasmas spectra produced during a wire array compression by a current up to  $\sim 3$  MA. The array 4847 consists of 60 tungsten wires with diameter  $6 \mu\text{m}$ . Its radius is 12 mm, height is 16.5 mm, linear mass is  $330 \mu\text{g}/\text{cm}$ , total mass is  $544.5 \mu\text{g}$ .

Computer modeling is aimed at reproducing of the pinch density and temperature distributions at consequent implosion stages. The appropriate data are used for radiation spectra calculations with reference to various observation points. This is done by means of a ray-tracing method.

The simulations of the pinch implosion are performed in a reduced domain representing a cylindrical sector 60 degrees with periodic boundary conditions posed at the side faces  $\varphi = 0$  and  $\varphi = \pi/3$ . Sector corresponds to  $1/6$  of the discharge chamber, which accounts for 10 wires assembly. The computational mesh consists of  $\sim 1$  billion cells and is refined near the axis. The electrodes are assumed ideal conductors. A boundary condition for a magnetic inductance is posed at the outer wall of the discharge chamber in the form  $B_\varphi = 2I/R$ , where  $R$  is a chamber radius and  $I$  is an electric current measured in the experiment.

In our computer model wires are substituted by a set of lines placed at initial wire positions. To account for a wire ablation we use an expression for a plasma production rate proposed in [8]:

$$\dot{m}(t) = \begin{cases} kB(t)^2, & t < t_\alpha, \\ \frac{kB(t_\alpha)^2}{M_0(1-\alpha)}(M_0 - m(t)), & t \geq t_\alpha. \end{cases}$$

Here  $\alpha = 0.5$ ,  $M_0$  is a total array mass,  $t_\alpha$  satisfies to a condition  $m(t_\alpha) = \alpha M_0$ , and  $B$  is global part of magnetic field at the wire position. The value of  $k$  is fitted to experimental observations indicating that usually a plasma generation cancels at a time  $\sim 10$  ns before a current reaches its maximum.

After 100 ns from the shot start the current pulse reaches almost half of its maximum value, and by this time about 16% of the array mass is ablated. Figure 1 shows plasma fluxes expiring from the remainder of wires and the gradual filling of the plasma space inside the array. As the plasma moves to the axis the shock wave is formed. An electron temperature at the shock front is  $\sim 40$  eV, the plasma velocity is  $\sim 10^7$  cm/s. By the time  $t \sim 130$  ns the wires evaporated completely, and the shock front is at a distance of 1 mm from the array axis. At a time  $t \sim 140$  ns the plasma reaches the axis. At this moment the radiation power profile relating to high energy photons reaches a ‘‘plateau’’ as seen from the figure 2.

At the time  $t = 166$  ns (figure 3, left), we observe some reduction in the radiation intensity (see figure 2), which can be explained so that the central pinch radiation is absorbed by trailing plasma masses. By this time the trailing masses are close enough to the intensely radiating near-axis plasma, but still are not merged with it.

Almost the entire mass is concentrated in the area with  $\sim 2$  mm in radius. The plasma density varies from  $10^{-3}$  to  $10^{-2}$  g/cm<sup>3</sup>, the density distribution along the radius takes the form  $\rho \sim 1/r$ . The electron temperature of the plasma is quite high and varies from 30–40 eV (at a distance of 2–3 mm from the axis) to  $\sim 70$  eV near the axis.

A moment  $t = 170$  ns from the beginning of the current pulse (figure 3, right) corresponds to the maximum plasma compression at the axis and the maximum of a radiation power (see figure 2). The central pinch (‘‘kernel’’) having a diameter of about 350 microns concentrates about 95% of the array material. Its maximum electron temperature in the kernel is 160 eV, the maximum density is  $\sim 0.66$  g/cm<sup>3</sup>, and the ionization degree is 25. Trailing masses are

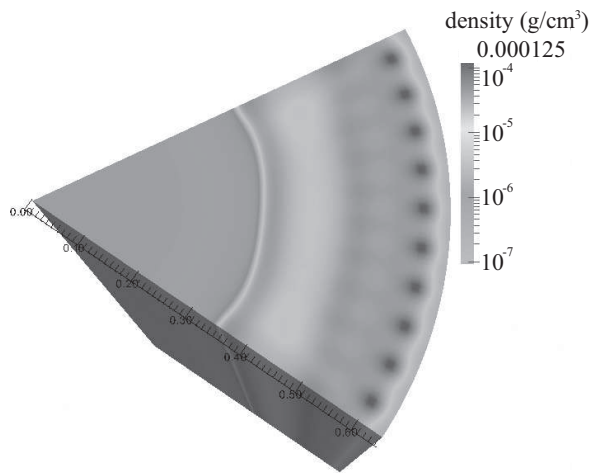


**Figure 1.** Calculated density distribution at  $t = 100$  ns.

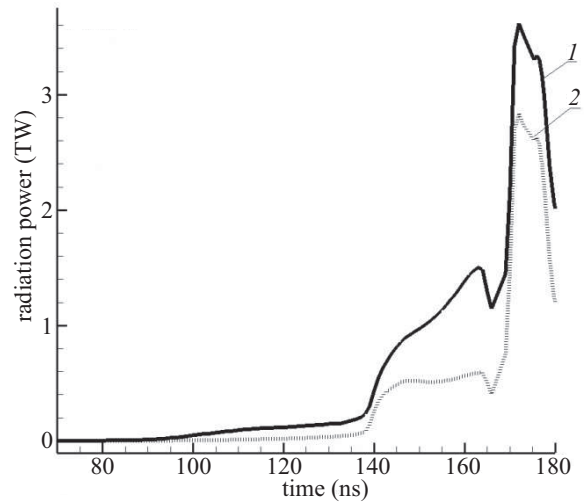


**Figure 2.** A radiation power as function of time, *1*—total radiation power over all spectral groups, *2*—radiation power of photons with energy higher than 100 eV.

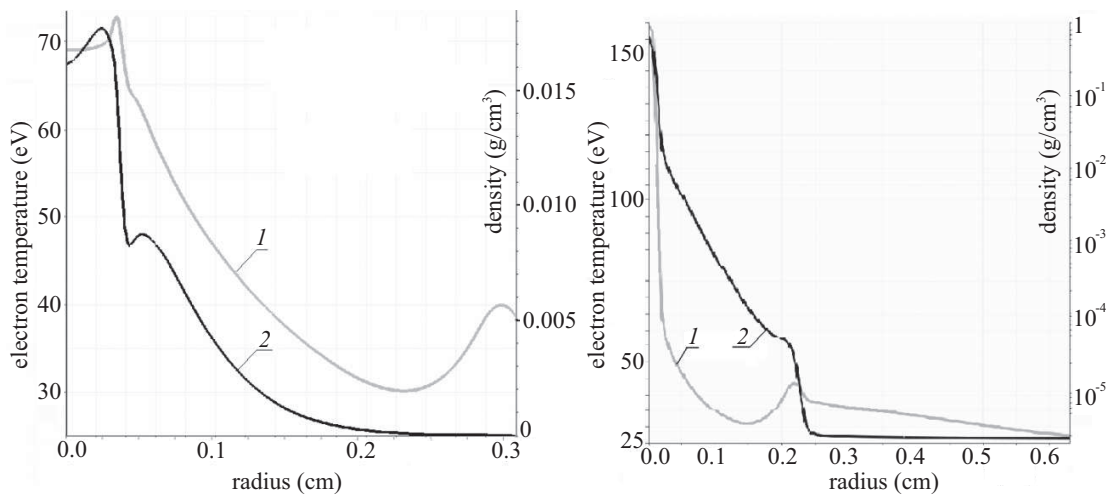


**Figure 3.** Radial distributions in the pinch: *1*—electron temperature and *2*—plasma density; the left figures are given for  $t = 166$  ns, and the right ones correspond to  $t = 170$  ns.

distributed over the domain with a radius of 2.5 mm at the following conditions: a density varies from  $2.1 \text{ g/cm}^3$  to  $4.1 \text{ g/cm}^3$ , an electron temperature is  $\sim 30 \text{ eV}$ , and a speed is  $\sim 2.2 \times 10^7 \text{ cm/s}$ .

During the pinch simulation, we calculate its total radiation power over all spectral groups dependent on time of the plasma compression. According to our calculations the total radiated energy is 45.5 kJ and the radiation power maximum reaches a value of 3.6 TW. The x-ray pulse duration at half-maximum of the peak power is  $\sim 10 \text{ ns}$ . The numerical results are in good agreement with the experimental data as concerns to the temporal profiles of the radiation power integrated over the pinch volume and spectral distributions of the photon energy, as indicators of the implosion.

A start point of the radiation power “plateau” (figure 2) corresponds to the time  $t \sim 140 \text{ ns}$

when the plasma precursor reaches the array axis. During the plateau existing, i. e. from  $t = 140$  ns to  $t = 170$  ns more than half the total radiation power relates to photons having energy of  $\sim 100$  eV. These photons are generated over the whole plasma volume having a density from  $4 \times 10^{-4}$  to  $3 \times 10^{-3}$  g/cm<sup>3</sup>, and electron temperature  $\sim 20$  eV. More hard photons are emitted from the pinch kernel where the plasma is heated up to 70–90 eV. The radiation power reaches its maximum at  $t = 170$  ns. This corresponds to the maximum plasma compression at the axis. Approximately 75% of the radiation power relates to photons with the energy from 100 to 400 eV.

#### 4. Simulations of time, spatial and angular resolved emission spectra of Z-pinch

Stagnation process of supersonically imploding tungsten plasma shell at the axis is accompanied by formation of stagnating shock wave. This shock wave converts kinetic energy of the shell into thermal energy of plasma and then into soft x-ray radiation. The latter one is reabsorbed considerably in outer layers. This process is responsible for formation of emission spectra. The radiative shock wave is supercritical one under the typical Angara-5-1 conditions, and its width is of the order of a few microns [3]. A hot plasma behind the supercritical shock front produces the short wave part of the soft x-ray spectrum that damped significantly due to absorption in the colder outer layers, whereas the long wave part of the spectrum is formed by the emission of these outer layers.

Simulation of the process considered above in cylindrical geometry is done by means of the radiative-hydrodynamic code RALEF-2D [9]. This code adopts spectrally resolved radiation transport using the characteristics-on-grid method. This allows simulation of angular resolved spectra on the global spherical system of rays. A sufficiently accurate calculation of a plasma hydrodynamics taking into account radiation-matter energy exchange is done with only eight-group approximation to a photon spectrum. A subsequent precise calculation of radiation distributions using the obtained fields of density, temperature etc. is implemented by splitting the total spectrum into  $\sim 2000$  groups. The initial conditions are taken in accordance with the results of the above MHD simulation.

Figure 4 shows emission spectra of the pinch depending on the angle of observation to the

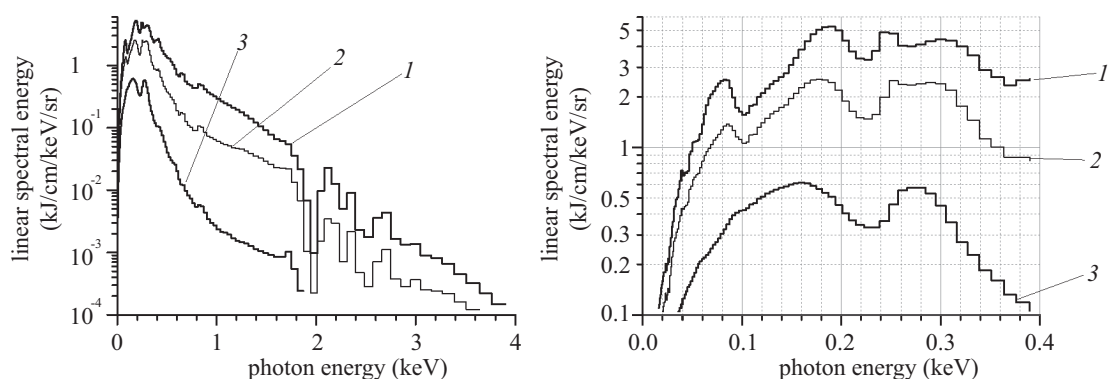


**Figure 4.** Spectral energies per unit length and per unit solid angle emitted at the angle  $90^\circ$  (1), at the angle  $30^\circ$  (2) and at the angle  $7.5^\circ$  (3) to the pinch axis. The right frame shows the same, but with larger scale close to maximum of the spectral density.

pinch axis. The spectral energy is normalized per unit length and per unit solid angle. We see that a part of the spectrum in the range of 0.7–2 keV is suppressed at smaller polar angles ( $7.5^\circ$  and  $30^\circ$ ). We may see also that spectral depression in the range between maximums at

80 and 190 keV is filled at small polar angles ( $7.5^\circ$ ). Besides, the spectral peak at 190 eV becomes spread and shifted to the region 160 eV. Two peaks at 250 and 300 eV merge in one smoother peak at 270 eV. The spectrum in the gross becomes softer at smaller angles to the pinch axis. Spectrally integrated energy as depended on this angle corresponds approximately to a Lambert's body.

Besides angular distributions of pinch emission, the full results of our simulation allows us to calculate spatial images of the pinch that could be obtained with an obscure placed at sufficiently large distance from the pinch perpendicular to the pinch axis. Our simulations imply that pinch is homogeneous along its axis. Hence simulated images depends only on distance along an imaginary observation slit. As a result our images are presented as plots of intensity versus this distance.

We have calculated spectral radiation composition using the data obtained for following spectral intervals: 1) 10–100 eV; 2) 100–1000 eV; 3) 500–2000 eV. These ranges correspond to different variants of experimental images registration.

Time integration of radiation of moving plasma shell spread significantly any details of calculated images. Nevertheless, the simulated images represented in figure 5 distinctly show:

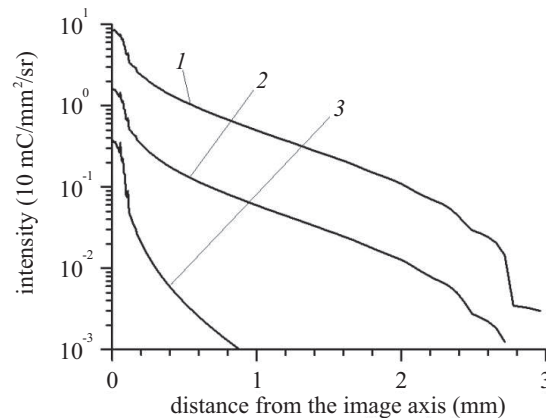


**Figure 5.** Time-integrated images of the pinch in different spectral intervals: 1—10–100 eV; 2—100–1000 eV; 3 — 500–2000 eV. Direction of viewing is perpendicular to the pinch axis.

- central peaks, that correspond spread by motion images of the shock wave, and that are damped due to propagation of radiation through absorbing shell; and
- relatively smoothly coming down pedestal, corresponding to emission of the outer layers heated by the radiation from the shock wave.

The cold outer layers move also. As a result its image is spread also. Shock wave image diameter is about 200  $\mu\text{m}$ . It contains about 30% radiation energy for the spectral intervals No. 1 and 2, and about 70% for the interval No. 3. Besides, image of the shell running against the axis obtained with the spectral interval No. 3 is significantly more compact, than for other filters. Surface brightness of outer layer images for intervals No. 1 and 2 becomes 10 times lower at 1.4 mm distance, whereas such decreasing for the interval No. 3 takes place at the radial distance about 0.6 mm.

## 5. Spectral data

The detailed tables of the absorption coefficients and emissivities for the tungsten plasma in a wide range of temperatures and densities are obtained with the help of the code THERMOS and the atomic database [10].

At the electrons density  $N_e = 10^{21} \text{ cm}^{-3}$ , the principal radiation lines correspond to the transitions 4d–4f (in the range lower than 100 eV) and 4d–5p (higher than 100 eV) in the tungsten ions with ionization  $\sim 14$ , which corresponds to the temperature 40 eV.

The ionization isotherms have been built from 1 to 316 eV in the logarithmic scale with 10 temperature points per order of value, for the densities from  $10^{-6} \text{ g/cm}^3$  to  $1 \text{ g/cm}^3$ . The performed analysis has shown that for the density  $1 \text{ g/cm}^3$  the radiating plasma is close to the equilibrium one.

The radiation spectra have been computed for a homogeneous layer of the tungsten plasma. The characteristic size of the layer is  $\rho L = 0.01 \text{ g/cm}^2$ , the electrons density is  $N_e = 10^{21} \text{ cm}^{-3}$  (the matter density changes from  $0.5 \text{ g/cm}^3$  till  $0.1 \text{ g/cm}^3$ ), for the various temperatures from 20 to 100 eV. The best agreement is achieved for the temperature 32 eV (figure 6, the left part). The grey line represents the experimental spectrum obtained in the experiment 4847.

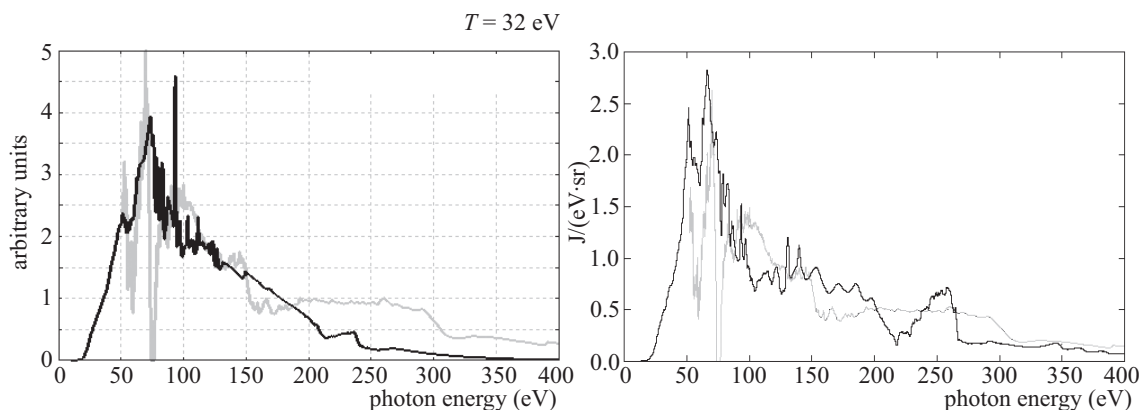


**Figure 6.** Computed spectrum (the black line): on the left part—for a homogeneous layer, on the right part—the one reconstructed for a given density and electron temperature distribution with the help of the tracing. The spectrum obtained in the experiment 4847 is reproduced by the grey line.

For the computation of the detailed radiation spectra, we have used the method of the tracing with the temperature and density distribution obtained from the gas-dynamic modelling. The transport equation in the cylindrical geometry was solving with the long characteristics method. The computation was performed with taking into account 1000 spectral groups. As a result, the temporally integrated spectra of the radiation of the pinch tungsten plasma are obtained. At the figure 6, the right part, we have represented the integrated radiation spectrum (the black line) obtained as a result of the modelling and observed from the direction at  $90^\circ$  with respect to the liner's axis, compared with the experimental spectrum with subtracted background (the grey line), obtained in the experiment 4847.

As a result of the tracing with a given density and electrons temperature distribution taking into account 1000 spectral groups, the dependence of the total radiation power on the time was computed. A similar dependence was obtained as a result of the MHD modelling discussed in Section 3, where a multigroup diffusion model with 20 spectral groups was used. An approximately twofold difference takes place between the total radiation power obtained by the tracing and by the gas-dynamical modelling. The reason may be that 20 groups is insufficient to describe the radiation absorption in plasma (the plasma seems to be too transparent when it is modelled with a mesh coarse with respect to the photons energy). On the other hand, since the result of the gas-dynamic modelling corresponds better to the experimental data (3.5 TW),



it apparently takes place some clarification of the outer wolfram plasma shell due to its high speed (Doppler effect), which has not been taken into account in the computations.

## 6. Conclusions

We studied the radiative properties of the tungsten wire-array Z-pinch. For this purposes 3D RMHD two temperature simulations of current-driven plasma implosion dynamics were carried out. We present the detailed model of the central pinch, which allowed to us to carry out the calculation of the intensity of the soft x-ray radiation with the temporal, spatial, angular and spectral resolution. The verification of the model was carried out by comparison with experimental data obtained in Angara-5-1. We compared the time dependencies of the integral radiation power over the whole plasma volume and the spectral distributions of the photon energy. We found good agreement between the numerical and experimental data.

We found that the influence of the trailing mass of tungsten plasma on the radiation intensity of the central part of the pinch in the radial direction can be explained by the absorption of radiation in the peripheral plasma layers.

The presented models and software tools can be used to forecast the experimental results with promising types of loads including specially profiled wire arrays aimed for formation of compact x-ray sources via quasi-3D plasma implosion.

## Acknowledgments

Simulations were performed using supercomputers Lomonosov (RSC MSU), MVS-100K (JSCC RAS) and K-100 (KIAM RAS). The work was supported by RFBR 11-02-01027-a, 13-02-00013-a, 14-01-00678-a, 15-01-06195-a, and by MD of RAS, grant OMN-3.

## References

- [1] Bolkhovitinov E A *et al.* 2012 *Plasma Phys. Rep.* **38** 824–32
- [2] Gasilov V *et al.* 2012 *Advances in Parallel Computing* **22** Applications, Tools and Techniques on the Road to Exascale Computing (IOS Press) 235–42
- [3] Basko M M, Sasorov P V, Murakami M, Novikov V G and Grushin A S 2012 *Plasma Phys. Control. Fusion* **54** 055003
- [4] Foord M E *et al.* 2004 *Phys. Rev. Lett.* **93** 055002
- [5] Vichev I Yu, Novikov V G and Solomyannaya A D 2009 *Mathematical Models and Computer Simulations* **1**(4) 470–81
- [6] Nikiforov A F, Novikov V G and Uvarov V B 2005 *Quantum-Statistical Models of Hot Dense Matter. Methods for Computation Opacity and Equation of State* (Basel, Berlin: Birkhauser Verlag)
- [7] Tkachenko S I, Mingaleev A R, Pikuz S A, Romanova V M, Khattatov T A, Shelkovenko T A, Ol'khovskaya O G, Gasilov V A and Kalinin Yu G 2012 *Plasma Phys. Rep.* **38** 1–11
- [8] Aleksandrov V V *et al.* 2001 *Plasma Phys. Rep.* **27** 89–109
- [9] Basko M M, Maruhn J and Tauschwitz An 2009 *J. Comp. Phys.* **228** 2175–93
- [10] Gu M F 2008 *Canad. J. Phys.* **86** 675–89